

Received:
17 August 2016Revised:
29 November 2016Accepted:
22 December 2016

© 2016 The Authors. Published by the British Institute of Radiology under the terms of the Creative Commons Attribution-NonCommercial 4.0 Unported License <http://creativecommons.org/licenses/by-nc/4.0/>, which permits unrestricted non-commercial reuse, provided the original author and source are credited.

Cite this article as:

Hutton BF, Occhipinti M, Kuehne A, Máthé D, Kovács N, Waiczies H, et al. Development of clinical simultaneous SPECT/MRI. *Br J Radiol* 2017; **90**: 20160690.

NUCLEAR MEDICINE: PHYSICS AND INSTRUMENTATION SPECIAL FEATURE REVIEW ARTICLE

Development of clinical simultaneous SPECT/MRI

¹BRIAN F HUTTON, PhD, ²MICHELE OCCHIPINTI, PhD, ³ANDRE KUEHNE, PhD, ^{4,5}DOMOKOS MÁTHÉ, PhD, DVM, ⁴NOÉMI KOVÁCS, MSc, ³HELMAR WAICZIES, PhD, ¹KJELL ERLANDSSON, PhD, ¹DEBORA SALVADO, MSc, ²MARCO CARMINATI, PhD, ²GIOVANNI L MONTAGNANI, MD, ⁶SUSAN C SHORT, MBBS, PhD, ^{7,8}LUISA OTTOBRINI, PhD, ⁹PIETER VAN MULLEKOM, ¹⁰CLAUDIO PIEMONTE, PhD, ¹¹TAMAS BUKKI, PhD, ¹¹ZOLTAN NYITRAI, MSc, ¹¹ZOLTAN PAPP, MSc, ¹¹KALMAN NAGY, PhD, ³THORALF NIENDORF, PhD, ¹²IRENE DE FRANCESCO, MD and ²CARLO FIORINI, PhD;
ON BEHALF OF THE INSERT CONSORTIUM

¹Institute of Nuclear Medicine, University College London (UCL), London, UK

²Dipartimento di Elettronica Informazione e Bioingegneria, Politecnico di Milano and Istituto Nazionale di Fisica Nucleare (INFN), Milan, Italy

³MRI.TOOLS GmbH, Berlin, Germany

⁴CROmed Ltd, Budapest, Hungary

⁵Department of Biophysics and Radiation Biology, Semmelweis University, Budapest, Hungary

⁶Faculty of Medicine and Health, University of Leeds, Leeds, UK

⁷Department of Medical-Surgical Pathophysiology and Transplants, University of Milan, Italy

⁸Institute for Molecular Bioimaging and Physiology (IBFM), National Council of Research (CNR), Milan, Italy

⁹Nuclear Fields, Vortum-Mullem, Netherlands

¹⁰Fondazione Bruno Kessler (FBK), Trento, Italy

¹¹Mediso Ltd, Budapest, Hungary

¹²Department of Oncology, University College London Hospitals NHS Foundation Trust, London

Address correspondence to: Prof Brian F Hutton

E-mail: b.hutton@ucl.ac.uk

ABSTRACT

There is increasing clinical use of combined positron emission tomography and MRI, but to date there has been no clinical system developed capable of simultaneous single-photon emission computed tomography (SPECT) and MRI. There has been development of preclinical systems, but there are several challenges faced by researchers who are developing a clinical prototype including the need for the system to be compact and stationary with MRI-compatible components. The limited work in this area is described with specific reference to the Integrated SPECT/MRI for Enhanced stratification in Radio-chemo Therapy (INSERT) project, which is at an advanced stage of developing a clinical prototype. Issues of SPECT/MRI compatibility are outlined and the clinical appeal of such a system is discussed, especially in the management of brain tumour treatment.

INTRODUCTION

Hybrid clinical systems with the combination of X-ray computed tomography (CT) and either single-photon emission computed tomography (SPECT) or positron emission tomography (PET) have been commercially available since 1999/2000 and have found important roles in clinical practice¹. The combination of clinical PET with magnetic resonance imaging (MRI) was more recent, necessitating the development of MRI-compatible components that support simultaneous acquisition.^{2–4} At the time of writing, however, the combination of SPECT and MRI in a simultaneous clinical system had yet to be achieved, although work is in progress to produce a functional prototype. This article provides an overview of this relatively new area of development and an insight into the challenges faced by researchers who are actively developing these systems. The coverage will summarize

the limited literature on SPECT/MRI technology, using as an example the clinical design adopted in an ongoing project (INSERT) funded under the European Commission FP7 framework. In this project, the researchers aimed to construct the world's first prototype clinical brain SPECT insert suitable for simultaneous use with an existing MRI. As in the case of the first clinical PET/MRI systems which were based on dedicated brain PET inserts, this system is a first step towards the potential development of a whole-body SPECT system which would have wider application.

There are some major technological challenges in achieving truly simultaneous SPECT/MRI, not least the need for MRI compatibility and MRI safety of components and electronics. Similar challenges have been faced by developers of PET/MRI, with the adoption of MRI-compatible readout as

replacement for the conventional photomultiplier tube (PMT).^{5,6} However, the need for compact detectors that include collimation and stationary tomographic acquisition impose additional constraints on the MRI-compatible SPECT system design. A sequential preclinical SPECT/MRI system is already commercially available and a number of preclinical synchronous SPECT/MRI experimental systems have been built in recent years, but these tend to rely on pinhole collimation with magnification, which mainly suits small objects.^{7–9} Developing a clinical system has required considerable innovation in many aspects of the design.

This article is structured as follows. The options for detector design are discussed, including a description of customized silicon photomultipliers (SiPMs) designed specifically for use in SPECT. The possible collimator designs and overall system design are discussed and MRI compatibility of components including electronics is considered. Finally, the potential applications of such systems are presented along with a brief discussion on the pros and cons of such a system.

SPECT DETECTORS FOR SIMULTANEOUS SPECT/MRI

In the case of the early development of PET/MRI, a compact brain PET insert was designed that could be utilized with an existing commercial MRI system.¹⁰ This then led to the development of more integrated systems suitable for whole body scanning.¹¹ A similar strategy for the development of SPECT/MRI can be adopted. One of the major constraints to be solved in the development of an integrated SPECT/MRI system is the design of a compact gamma detection module which exhibits mutual compatibility with commercial MRI scanners. PMTs are the photodetectors most commonly used in conventional SPECT systems. Unfortunately, PMT arrays are too bulky to be fitted inside an MRI bore and their performance is severely affected by the high magnetic field and the pulsed magnetic field gradients used in MRI. Several solutions have been suggested. The first approach considers the placement of magnetic-sensitive devices, such as PMTs, far enough from the MRI apparatus, with light carried from the scintillators to the photo detectors through long optical fibres.^{12,13} Another approach is based on the adoption of either pixelated solid-state detectors [e.g. cadmium telluride (CdTe), cadmium zinc telluride (CdZnTe or CZT)]^{7,14–16} or inorganic scintillators coupled to solid-state photodetectors (e.g. avalanche photodiodes or SiPMs).^{17–19} Digital SiPM technology has also been developed, where on-chip circuitry enables fast, accurate photon counting and well-defined timing.²⁰ In combination with compact readout electronics, these solutions provide compatibility with high magnetic fields and compact designs that are suitable for use within MRI bore sizes of 60–70 cm commonly used in clinical practice.

A strong case has been made for the adoption of SPECT/MRI for preclinical use.¹⁴ In most of the experimental synchronous preclinical SPECT/MRI systems under study, arrays of CdTe or CdZnTe (CZT) gamma detectors are employed,^{21,22} Similar solid-state technology is finding increasing use in clinical SPECT systems being used for cardiac imaging,^{23,24} scintimammography²⁵ and, more recently, whole-body SPECT imaging.²⁶ As regards compatibility with MRI, preliminary investigations on CdTe and CZT have shown

that a shift of the signal charge inside the detector caused by Lorentz forces takes place and this phenomenon requires correction to improve the detector response so as to achieve a high resolution.⁹

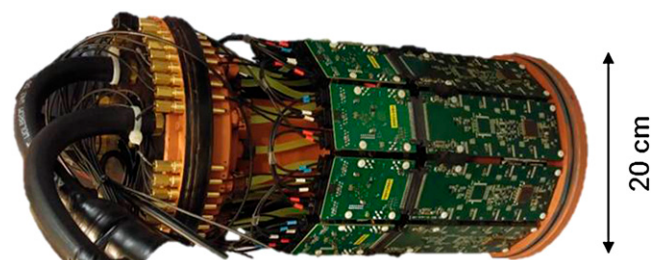
An alternative for use in SPECT/MRI is the employment of SiPMs to read out the light emitted by inorganic scintillators.²⁷ Beyond the wide success of such detectors in MR-compatible PET systems,^{28–30} there are several SPECT development projects reported in the literature, exploring SiPM-based gamma detector modules.^{31–34} The goal of these researchers was to produce compact gamma cameras for use in surgery or small organ imaging. These systems have not normally been developed specifically for MRI compatibility and are not tomographic, but similar compact technology could be adapted for use in synchronous SPECT/MRI. SiPMs show no intrinsic sensitivity to magnetic fields, an important argument for the usage of a SiPM-based gamma camera in combination with MRI.⁶ Although the energy resolution of a scintillation-based system is typically inferior to that offered by CdTe and CZT, it is still adequate to potentially allow specific clinically important multi-radionuclide acquisitions (e.g. ^{99m}Tc and ¹¹¹In, ^{99m}Tc and ²⁰¹Tl).

A disadvantage of pixelated detectors is that they involve direct readout for each pixel; the number increases as the pixel size is decreased. In comparison, a SiPM readout system with multiplexing requires a relatively small number of direct electrical connections, since the readout units are quite large compared with the resolution (at least an order of magnitude larger). This opens the possibility to reach a given spatial resolution with a significant reduction in the number of electronic readout channels (a factor of 100) compared with a pixelated detector with the pixel size equal to the desired resolution.³⁸ This advantage will be particularly important in the translation of this technology for clinical application. For a scintillator in combination with SiPMs, sufficiently high intrinsic spatial resolution is achievable (approximately 1 mm) to enable compact SPECT designs, taking advantage of multiple apertures with minification.^{35–37}

SPECT/MRI SYSTEM DESIGN

Sequential SPECT and MRI has been performed with small-animal SPECT adjacent to a low-field (0.1 T) MRI system,³⁹ a solution still limited by the lack of simultaneity and by the need for a low magnetic field. Several groups have designed MRI-compatible preclinical systems. The design of an MRI-compatible SPECT system for mouse brain imaging has been

Figure 1. A full preclinical ring populated with 10 gamma detection modules. The mechanical structure also supports the cooling distribution tubes and the power and optical communication lines. The overall diameter of the insert is 20 cm.



presented together with results of the effect of SPECT and MRI components on each other.⁷ This early development led to more recent construction of an ultrahigh-resolution stationary MRI-compatible SPECT system for small animal imaging, based on CdTe/CdZnTe detectors.²² Further preclinical systems have been developed through academic/industrial collaborations and the SPECT–MRI interaction has been evaluated.^{8,40–42} A preclinical SPECT system has been designed using Lutetium Yttrium Orthosilicate and digital SiPM;⁴³ the high-density detector enables use of a thin detector for SPECT with the potential to reduce depth of interaction effects that are common with pinhole collimation. However, the light output is somewhat compromised for low-energy gamma emitters. A preclinical prototype based on SiPM readout has also been developed in the INSERT project,⁴⁴ with modular detectors that also suit a clinical SPECT design (Figure 1). First images from the preclinical system have been recently demonstrated.¹⁰

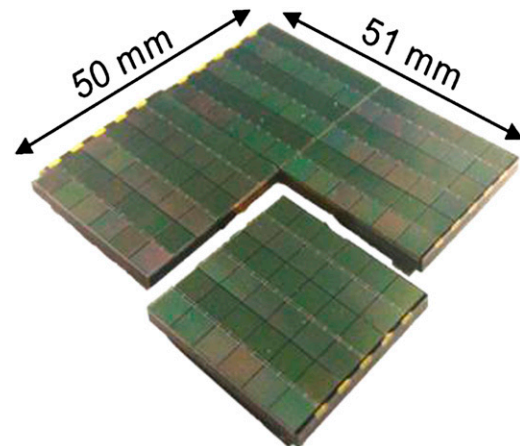
At the time of writing, the only commercially available preclinical SPECT/MRI system (nanoScan® SPECT/MRI 1.0 T; Mediso, Budapest, Hungary) was an inline system that uses a combination of high-resolution multipinhole apertures, a PMT-based conventional SPECT detection module and a specially developed shielding system combined with a self-shielded 1.0 T permanent magnet. This combination has been proven to yield a high SPECT image quality and high-resolution imaging possibilities coupled with a user-friendly and biologically relevant series of MRI sequences. However, inline SPECT/MRI still lacks the advantages presented by synchronous SPECT and MRI acquisition.

At the time of writing, there was publication of only one clinical SPECT/MRI under construction (INSERT)²⁵ dedicated to human brain imaging. The system has been designed using stationary rings of detector modules, designed so as to minimize variation in the components when translating from the preclinical to the clinical configuration. The electronic board, for SiPM signal processing and transmission through optical fibres, also provides mechanical support for a modular number of compact SiPM arrays supplied by FBK, Trento, Italy.⁴⁴ The SiPM arrays are arranged in tiles to cover the required detector area: $5 \times 5 \text{ cm}^2$ for the preclinical configuration and $10 \times 5 \text{ cm}^2$ in the clinical case (Figure 2). An 8-mm-thick CsI(Tl) monolithic scintillator is optically coupled over the overall SiPM matrix surface.

The detection module performance is mainly determined by the amount of light detected by the SiPM array. Since SPECT involves use of radionuclides with relatively low emission energy, a low amount of light is generated for any scintillation event. Thus, the following design principles have been employed:

- (1) A CsI(Tl) scintillator has been adopted. CsI has a high light output and, although it is one of the slowest inorganic crystals, the timing performance of the camera is sufficient to handle the expected clinical count rate.
- (2) The gaps between SiPM cells have been minimized through a set of smart strategies in SiPM alignment.⁴⁴ As a result, loss in light detection has been significantly reduced.

Figure 2. The three-side-tiltable silicon photomultiplier arrays composing the planar detector field of view in the preclinical case. The dead detection area of the single array has been minimized to increase the amount of luminous signal collected.



- (3) SiPM technology with optimal optical detection efficiency has been chosen, specifically adapted to the optical wavelength for CsI scintillation.

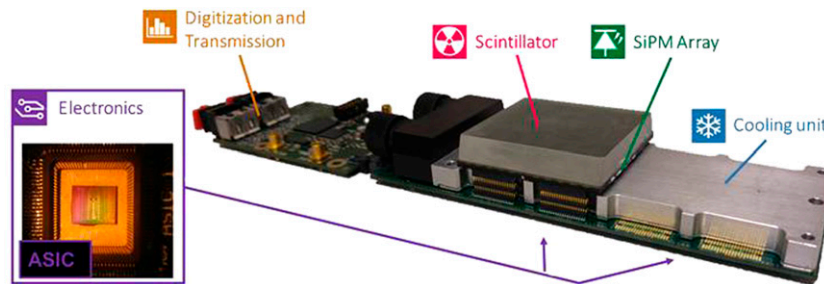
At room temperature, the presence of thermal noise results in deterioration of the energy resolution, necessitating cooling of the SiPM array. The detector module therefore incorporates a compact 8-mm-thick cooling block made of MR-compatible thermoplastic (Coolpoly®; Cool Polymers, North Kingstown, RI), placed between the SiPM array and the electronic readout board and designed to ensure uniform temperature control over the SiPM area (Figure 3). A glycol–water mixture is circulated to maintain the operating temperature of 0 °C. Image quality over the single gamma detection module has been tested with ^{99m}Tc (Figure 4). The intrinsic spatial resolution of the device is approximately 1.0 mm full width at half maximum over a planar field of view (FOV) of slightly greater than $4 \times 4 \text{ cm}^2$.

The clinical system design is illustrated in Figure 5. This is based on use of 20 detector modules arranged in a partial ring, designed to maximize the patient aperture with minimal alteration to the existing patient bed. The key to development has been the choice of a collimator, which has been designed to provide maximum axial coverage and optimal sensitivity, while maintaining reconstructed resolution so as to be similar to conventional gamma camera SPECT. The reason for this target was the intention to explore the use of the technology to characterize and evaluate treatment in well-identified brain tumours rather than to optimize detection of small abnormalities.

COLLIMATORS FOR CLINICAL SPECT SYSTEMS

The design of a compact clinical system is markedly different from the typical preclinical designs where multipinhole collimators usually take advantage of magnification to achieve superior resolution. With improvement in intrinsic resolution, the degree of magnification can be reduced so as to achieve the desired compact design. Similar designs have been

Figure 3. INSERT gamma camera configured for preclinical SPECT. In the violet box, the 36-channel application-specific integrated circuit (ASIC) for signal readout and filtering is depicted. Digitized SPECT signals are transmitted through optical fibres. Temperature is stabilized at 0 °C by the cooling unit (an aluminium version of the unit is depicted). SiPM, silicon photomultiplier.



adopted to achieve superior resolution for clinical brain SPECT [(G-SPECT; MiLabs, Utrecht, Netherlands) (AnyScan Trio; Mediso)]; however, these systems are not compact. Instead, the improvement of intrinsic resolution using the new technology can be used to advantage by adopting minification as opposed to magnification so that the resolution is effectively traded against compactness, to achieve similar performance to a conventional gamma camera SPECT system.

The main challenges in collimator design are to construct a compact system with sufficient angular sampling to permit stationary acquisition (avoiding detector movement is highly desirable for simultaneous SPECT/MRI acquisition). Van Audenhaege *et al*⁴⁵ proposed a design for a multipinhole collimator for performing clinical brain SPECT studies using an existing PET scanner. The collimator was equipped with a shutter mechanism, in order to eliminate the need for rotation; however, the prototype was not MR-compatible. Preclinical systems usually utilize multipinhole collimators;^{46,47} but, for a compact clinical system, preference was given to utilizing a multislit-slat collimator (Figure 6), which incorporates several novel features. The slits are located internal to the slats so as to achieve the desired minification without compromising slat length (which controls the axial resolution/sensitivity trade-off).

Multiple short slits are employed to improve the angular sampling and slits are shared across detectors so as to accommodate the desired FOV. The resulting collimator³⁷ demonstrates higher sensitivity than alternative multipinhole collimators and also improves on fan beam collimation, which is commonly used on conventional SPECT.

A further consideration in collimator design is the choice of material and the avoidance of features which might result in induced eddy currents. The rapid switching of gradient coils induces spatially and temporally varying eddy currents within the conducting structures of the MRI scanner and in the collimator required for SPECT, which typically has a high conductivity. The undesired magnetic field produced by these eddy currents opposes and distorts the linear gradient fields in the region of interest, which results in image artefacts.⁴⁸ Other effects concern the thermal load in the cryostat of the superconducting magnet, which may lead to increased boil-off of the cryogenics (can even cause magnetic quenching in extreme cases) and acoustic noise due to their interaction with the B_0 field.⁴⁹ The material traditionally used for collimators and shielding is lead, strengthened by various impurities that tend to be ferromagnetic. The alternative is to use tungsten and several groups have developed tungsten/epoxy composites in an attempt to

Figure 4. Planar irradiation profile for a 5 × 5 cm field of view of the preclinical INSERT detector module. (a) A lead grid of holes (0.5 mm in diameter, 2 mm pitch) is employed to collimate the gamma rays. (b) Experimental result for ^{99m}Tc: the event coordinates were reconstructed using a maximum likelihood method. FWHM, full width at half maximum.

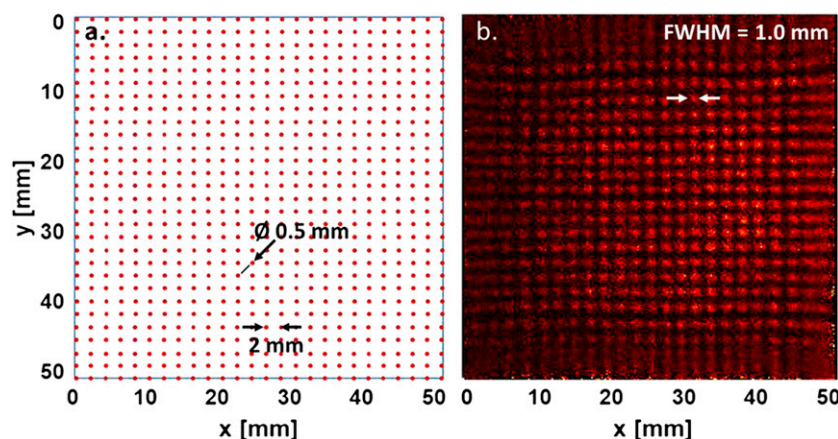
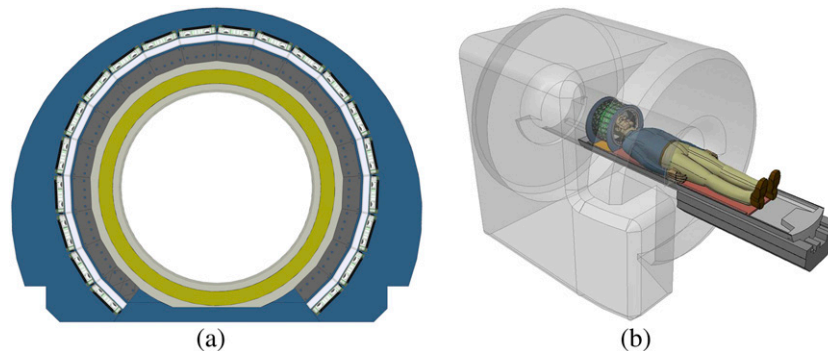


Figure 5. (a) Schematic diagram of the clinical system design with a partial ring of 20 detectors. The patient aperture of 33 cm accommodates the MRI receiver/transmitter head coil. (b) Schematic of complete SPECT insert in the MRI system.



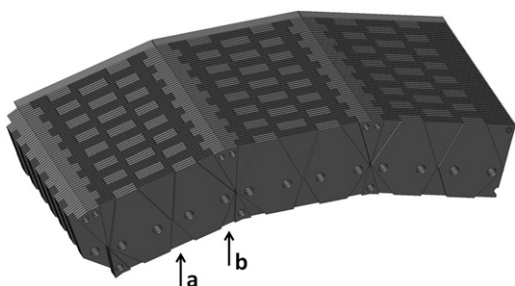
reduce eddy currents while maintaining stopping power.⁵⁰ This strategy works well for radiation shielding, with attenuation approaching that of lead being possible. However, the composite material tends to be brittle and easily broken and so not suitable for fine collimator components.

Various strategies can be employed in the design of pinhole collimators to reduce the incidence of eddy currents, *e.g.* segmenting the collimator into smaller subsections while avoiding any possible penetration.⁵¹ Manufacturing the resulting complex parts is greatly aided by recent developments in additive manufacturing.⁵² In the case of already complex multicomponent tungsten collimators (*e.g.* multislit-slat collimators), induced eddy currents appear to be acceptably small.

SPECT/MRI COMPATIBILITY

The technical challenges of integrating a SPECT insert with a clinical MRI system relate primarily to potential interferences between both modalities. These interferences might compromise MR safety and MR compatibility. The requirements of MR safety are met if the SPECT device poses no known hazards in a specified MRI environment with specified conditions of use. Conditions that define the MRI environment include static magnetic field strength, spatial magnetic field gradient, time-varying

Figure 6. Multislit-slat collimator corresponding to three detector units. The collimator consists of slats in the axial direction and an array of short slits with their apertures internal to the collimator surface. The figure shows a central slit (a) for each of the three subsections plus slits that are shared across adjacent detectors (b).



magnetic fields and radiofrequency (RF) power deposition. Additional conditions, including specific configurations of the SPECT device (*e.g.* routing of leads and power lines), may be required. MR compatibility indicates that a SPECT device, when used in the MR environment, does not significantly reduce the quality of the diagnostic information *via* the formation of MR signal and image artefacts and that its operation will not be detrimentally affected by the MR device.

Mutual SPECT/MRI safety and compatibility issues may arise from:

- static magnetic fields (B_0): interference with the B_0 spatial gradient can cause displacement and torque of objects moved into the MR environment. This displacement force is responsible for the projectile effect that continues to cause accidents in the MR environment. Diagnostic MRI and MR spectroscopy require a B_0 uniformity of ≤ 1 ppm and foreign objects such as bulk collimators, SPECT detector modules and large bundles of lead placed in the MR magnet run the potential to perturb B_0 . The static magnetic field might also induce susceptibility effects which bear the risk of spoiling the MR signal and image quality if placed close to the FOV used for MRI. Sensitivity to B_0 might also cause malfunction and dysfunction of the SPECT device owing to electromagnetic interference with its electronics and detectors.
- Switching magnetic fields ($dB/dt: \leq 200$ mT/m/ms): switching magnetic fields can cause movement, frequency shift and temperature rise owing to eddy currents induced in conductive system components (cables, collimator, cooling blocks, means of shielding, scintillators etc.) placed inside the magnet bore equipped with a gradient coil. Pulsed magnetic field gradients might also interfere with the electronic circuits and detectors of the SPECT device, disturbing the low amplitude signals within the SPECT acquisition chain (application-specific integrated circuit, data acquisition board etc.).
- RF energy transmission (B_1^+): RF transmission can induce temperature rise and functionality disturbances owing to RF power deposition. RF might also interfere with the electronics and detectors of the SPECT device owing to RF shielding deficits. Any RF emission of the SPECT device (for example: power supplies or preamplifier electronics) bears the potential

to interfere with the MR device and compromise its (diagnostic) functionality through RF-induced artefacts.

- Movement and flow: mechanical movement of components of the SPECT device can cause MR frequency shift owing to eddy currents. Flow (for example: cooling fluids) in the FOV to be imaged can cause MRI artefacts that present an impediment for diagnostic image quality. The implications feed into the (stationary) collimator design and the cooling strategy used for heat extraction from the SiPMs thermal pads.

The literature primarily reports on evaluation of MR compatibility and safety of instruments for interventional MR procedures^{53–56} and provides guidance for standardized test procedures^{57–60} that mainly focus on passive devices. A SPECT insert is an active device that differs from interventional MR devices/applications in many aspects. For the design of a synchronous clinical setup, careful considerations need to be made to reduce if not eliminate electromagnetic coupling between the MR and SPECT device with the goal to assure SPECT/MR compatibility. These considerations should include legal regulations⁶¹ and established norms,^{62,63} but should also build upon a close interdisciplinary team work involving experts in electrical engineering, SPECT manufacturing, RF antenna design, MR physics, nuclear medicine and radiology. As a minimum, procedures for ensuring MR safety and compatibility should include the following assessments.

Hard magnetic materials

Hard magnetic materials (also known as permanent magnets) including high carbon steels, barium, ferrite, alnico, samarium–cobalt alloys etc. are not MR-safe and should be strictly banned from any clinical SPECT design. This test can be conveniently performed by measuring the attraction force of a piece of metal plate placed in the vicinity of the material under investigation.

Soft magnetic materials

Soft magnetic materials are not magnetized if not placed in the vicinity of a magnetic field. However, their susceptibility is very large and they exhibit forces and torques in the presence of a strong magnetic field of a clinical MR scanner.⁶⁴ The test for soft magnetic materials is performed according to the American Section of the International Association for Testing Materials (ASTM) Standard F2052-06.⁵⁷ For example, WNiFe collimator materials (alloy 1: $\rho = 17.6 \text{ g cm}^{-3}$, W = 93%, Ni = 5%, Fe = 2%; alloy 2: $\rho = 18.0 \text{ g cm}^{-3}$, W = 95%, Ni = 3.5%, Fe = 1.5%; Nuclear Fields International, Vortum-Mullem, Netherlands) were found to be ferromagnetic and excluded from the collimator design. In comparison, collimator samples of polyimide/tungsten ($\rho = 11.0 \text{ g cm}^{-3}$), lead + 4% antimony ($\rho = 11.03 \text{ g cm}^{-3}$), lead ($\rho = 11.3 \text{ g cm}^{-3}$) and tungsten ($\rho = 19.3 \text{ g cm}^{-3}$) are non-magnetic.

Non-magnetic materials

Non-magnetic materials exhibit small magnetic susceptibility χ so that no forces and torques are apparent when placed in a static magnetic field. To avoid any B_0 perturbation induced by the magnetic susceptibility of the SPECT insert, the ideal magnetic

susceptibility would be $\chi_{\text{SPECT insert}} = \chi_{\text{air}} = 0.36 \times 10^{-6}$ which is hard to achieve in practice.⁶⁴ The effects of magnetization induced by non-magnetic materials/objects used for the SPECT insert are largest at the surface of the object. Therefore, it is prudent to place all components of the SPECT system outside of the FOV of the MR system for avoiding susceptibility gradient-induced artefacts. The tests for magnetic susceptibility are based on the ASTM Standard F2119-07⁵⁸ and on the study of Wendt.⁶⁵ To achieve this goal, a material probe together with a reference probe (e.g. copper) is placed in close proximity to an imaging phantom⁶⁵ filled with a solution.⁵⁸ MR scans are performed for multiple orientations to evaluate the severity and extent of magnetic field distortion and susceptibility artefacts induced by the material under investigation vs the reference probe (Figure 7).

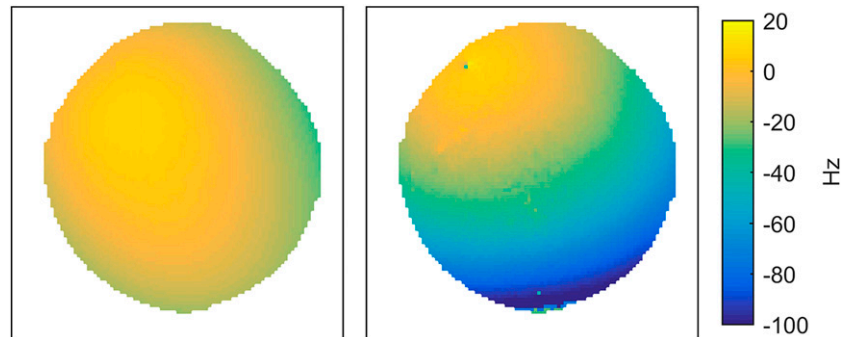
Frequency shift and free induction decay attenuation due to eddy currents induced by pulsed magnetic field gradients

Local eddy currents disturb B_0 homogeneity resulting in frequency shift, T_2^* relaxation time shortening and free induction decay (FID) attenuation. For eddy current and frequency assessment, a reference FID/spectrum is acquired for an agarose phantom. For comparison, the object under test is placed in the magnet (resembling its position in the SPECT insert) followed by the acquisition of a test FID/spectrum. For both sets of measurements, the delay between the pulsed magnetic field gradient and the FID acquisition is varied to determine the eddy current time constant (Figure 8). Eddy current considerations have major implications for the design of the heat exchangers, since commonly employed copper heat exchangers (which exhibit very good thermal conductivity 401 W/mK^{-1}) cannot be implemented. To overcome this limitation, thermally conductive non-metallic materials, such as ceramic material SHAPAL™ (Precision Ceramics, Birmingham, UK) (thermal conductivity 92 W/mK^{-1}) or thermally conductive plastic CoolPoly® D5506 (Cool Polymers, North Kingstown, RI) (thermal conductivity 10 W/mK^{-1}), are alternative candidates for the cooling block material. The latter is less costly and can be easily modelled in complex forms with robust and reliable outcomes.

Heat extraction and spurious MR signals

From the MR perspective, air cooling can be considered as an ideal candidate for heat extraction from the SiPM thermal pads, since air does not induce spurious MR signals. However, air cooling constitutes a severe challenge for flow and temperature stabilization needed for the SiPM performance. For this reason, a water and glycol mixture (40–60%) is used for heat extraction from the cooling block. To reduce spurious MR signals, the RF coil is shielded. Also, the tubes supplying and draining the heating blocks need to be routed outside of the excitation field of the RF coil to avoid spurious signals in the MR images. The remaining concern is spurious MR signals due to aliasing of the parasitic signal obtained from the cooling fluid outside of the FOV into the FOV. This artefact is induced by parasitic excitation of regions outside of the FOV owing to the non-linearity of the gradient coil, and commonly called “third arm artefact”. Parasitic excitation can be addressed by limiting

Figure 7. Magnetic field distortion inside a uniform phantom due to the presence of a collimator block (polyimide/tungsten, $\rho = 11.0 \text{ g cm}^{-3}$) tested for the clinical SPECT/MRI setup. The left image shows a uniform static magnetic field in the absence of the collimator block. For this setup, a magnetic field dispersion (Δf) of approximately 20 Hz was obtained across the slice. After placing the collimator block in close vicinity to the phantom lower right corner, the static magnetic field is significantly distorted (right) which manifests itself by field dispersion across the slice of $\Delta f \approx 120 \text{ Hz}$.



the range of excitation and reception of the RF coil using a dome-shaped design or by employing a bird cage design tailored to the brain.

Mechanical vibration due to pulsed magnetic fields gradients

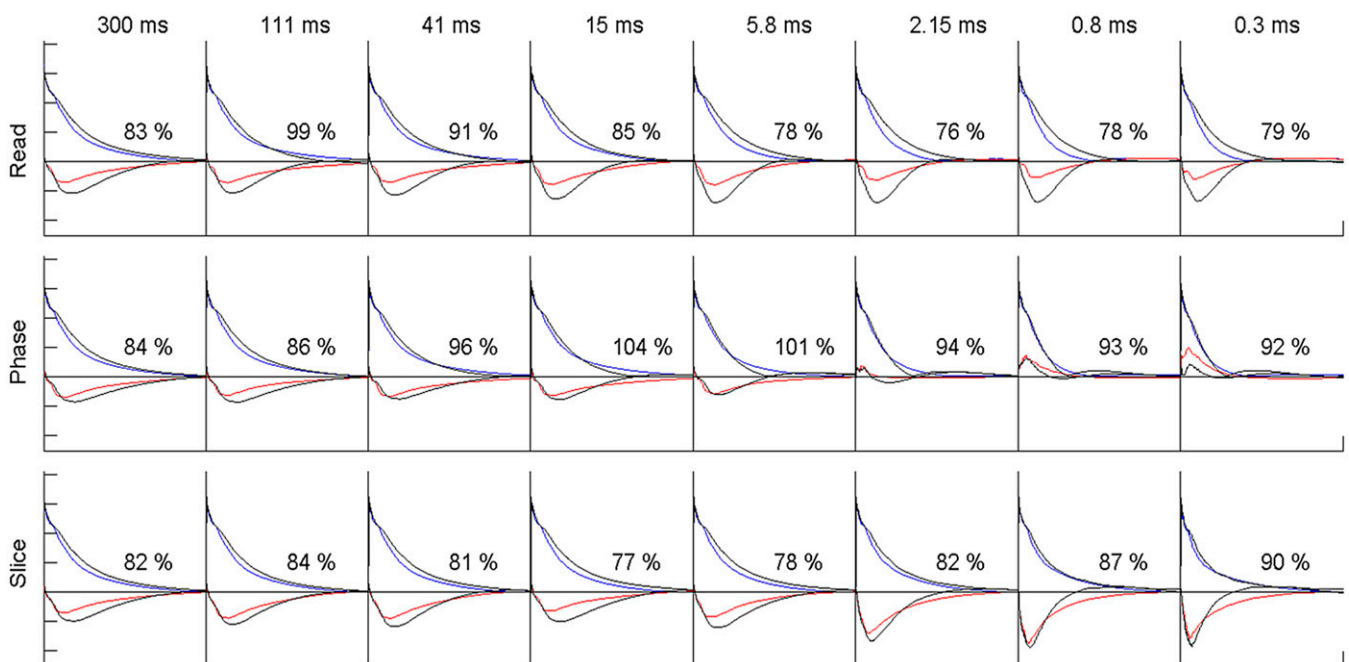
The literature is short of a standardized test given by ASTM or other bodies that is tailored for examining mechanical vibration induced by a device incorporated or inserted in an MR scanner. Careful considerations should include the use of pressure and acceleration sensors. It is advised that the eigenfrequencies of the SPECT components should not match the frequencies of the

magnetic field gradient-switching schemes used for MRI to avoid strong coupling.

Temperature changes due to pulsed magnetic fields gradients

Under normal conditions, the heating due to pulsed magnetic field gradients in the kilohertz frequency range is negligible.⁶⁶ This may change if bulky electrically conductive objects (collimator, cooling blocks, application-specific integrated circuit etc.) are placed in the MR scanner. For temperature monitoring, an object under test is placed either in air or in a gel phantom^{59,67} and positioned in the MR scanner according to its

Figure 8. An example of eddy current assessment using a reference free induction decay (FID) (black line) obtained for an agarose phantom and pulsed magnetic field gradients placed along the read, phase and slice direction. For comparison, the object under test [polyimide/tungsten sample ($\rho = 11.0 \text{ g cm}^{-3}$)] was placed in the magnet (resembling its position in the SPECT insert) followed by the acquisition of a test FID (blue and red lines). For assessment of the eddy current time constants, the delay between the pulsed magnetic field gradient and the FID acquisition was varied between 0.3 and 300 ms.



position within the SPECT system. Temperature probes are attached to the object and positioned in its vicinity. Pulsed magnetic field gradients are applied using clinical MR protocols including fast spin-echo, fast gradient-echo and echoplanar imaging sequences for fast and high duty cycle switching paradigms.

Pulsed gradient fields

Pulsed gradient fields can induce electrical voltages on the SPECT device components as well as on all electrical cables connected to them. These voltage spikes interfere with device operation and can cause measurement artefacts in the form of spectral distortions and can even lead to a complete operational failure if voltages become too high. Electromagnetic simulations and bench measurements using pulsed magnetic field generators such as toroidal coils are performed to test problematic configurations and identify possible mitigation measures.

SPECT/MR interferences due to radiofrequency transmission/emission

This compatibility issue can be twofold: (i) interference of RF coil transmission with the functionality of the SPECT modules and (ii) interference of RF emission induced by the SPECT device with the RF chain of the MR scanner. To reduce RF interferences caused by the SPECT module, it needs to be electromagnetic compatibility shielded. Efficiency of electromagnetic compatibility shielding can be evaluated by placing the components of the SPECT electronics in a shielded box followed by measurements of RF spectra outside of the box (Figure 9). The RF coil itself is shielded and, in addition, is separated from the active components of the SPECT system by a collimator, which reduces (if not eliminates) RF interference with the SPECT device. For the evaluation of MRI/SPECT interferences, it is prudent to use a transmitted RF power that exceeds the limits given by the International Electrotechnical Commission guidelines by a factor of 3. For the assessment of SPECT/MRI interference, noise figures are acquired. For this purpose, the component under investigation is placed in the MR system with the collimator (or alternative shielding) being installed. An RF

coil and an MRI phantom are placed inside the collimator. A noise scan and clinical imaging protocol are performed, while the component under test is in operation. These scans are benchmarked against reference data acquired without the component under investigation in the bore.

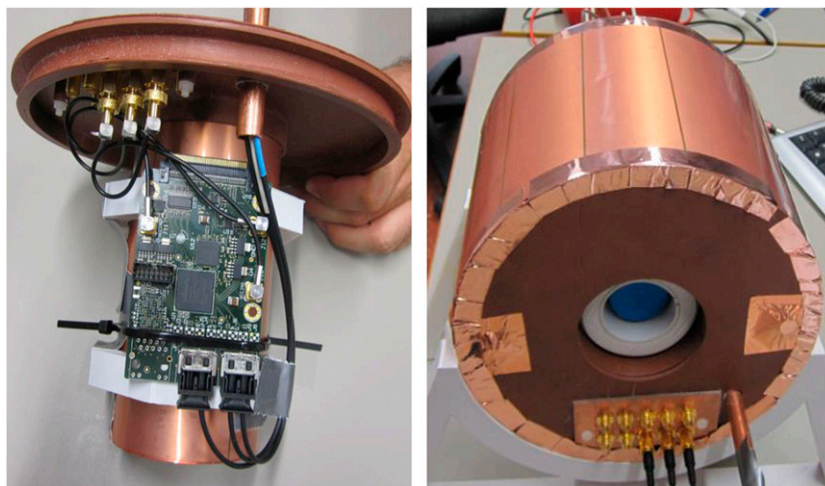
Radiofrequency heating induced by the radiofrequency transmission

In current clinical MR scanners, integrated large-volume body RF coils are commonly used for RF excitation. The large-volume excitation bodes well for a uniform transmission field. Yet, this approach is not suitable for a clinical SPECT/MR setup owing to the RF shielding provided by the collimator and other components of the SPECT insert. Instead, a small-volume transmit/receive RF coil tailored to the geometry of an average head and positioned inside the SPECT insert is employed. The RF power applied to this RF coil needs to be limited to meet the RF power deposition and specific absorption rate limits governed by the International Electrotechnical Commission guidelines.⁶⁸ For this purpose, careful electromagnetic field simulations need to be conducted in human voxel models. For validation, transmission field distributions obtained from these simulations need to be benchmarked against experimental B_1^+ maps.^{69,70} Since the integrated SPECT module is placed outside of the RF coil, it is unlikely that the head coil of the MR scanner would induce heating into the SPECT module that might cause a compatibility issue.

Potential applications of clinical SPECT/MRI

In general, it is the authors' opinion that multi-radionuclide SPECT imaging with well-established radiopharmaceutical tracers of a variety of metabolic and molecular features could indeed provide useful synergies with function-related physiometabolic MRI and spectroscopy including X-nuclei MRI. Owing to the massively multiarray possibilities of the resulting images, synchronous SPECT/MRI realizes insights hereto impossible for any other type of hybrid imaging methodologies (including PET/MRI). As nowadays fully quantitative SPECT reconstruction can be achieved, synchronous SPECT/MRI

Figure 9. A data acquisition board mounted inside the electromagnetic compatibility shielding test box for the evaluation of the SPECT/MRI interference due to radiofrequency emission (left). Closed test box being fully shielded (right).



equipped with high temporal resolution acquisition will be the method of choice for personalized therapy guidance and “radiomics”-based decisions (*i.e.* use of imaging parameters as a surrogate for reading out tumour biology).

One goal of the current synchronous SPECT/MRI development is to aid in the clinical management of patients with brain tumours. Assessment of treatment response in patients with glioma is currently extremely challenging. Anatomical and contrast-enhanced MRI remains the standard imaging modality at follow-up, but is associated with well-documented problems in ascertaining response to treatment, particularly at early time points owing to the phenomenon of pseudoprogression⁷¹ associated with inflammation. Currently, patients with imaging findings that suggest progression or pseudoprogression are managed expectantly, since the only approach to confirming the diagnosis is through continued clinical and radiological follow-up. It is notable that fluorodeoxyglucose (¹⁸F-FDG) imaging has not proven useful for this indication, although amino acid tracers may be more relevant and are still under investigation in this setting.^{72,73} Hence, based on current imaging approaches, patients who have true progression may be denied access to alternative treatments early and patients who will have an ultimately favourable outcome cannot be reassured. In the context of pseudoprogression, the earlier the imaging is carried out following treatment, the less useful the data tend to be and to date, there have been no successful approaches to monitor these patients during treatment. This is despite the fact that real-time assessment of treatment response, for example during radiotherapy or adjuvant chemotherapy, could allow for selection of patients for treatment intensification at the time when treatment is likely to be most effective.

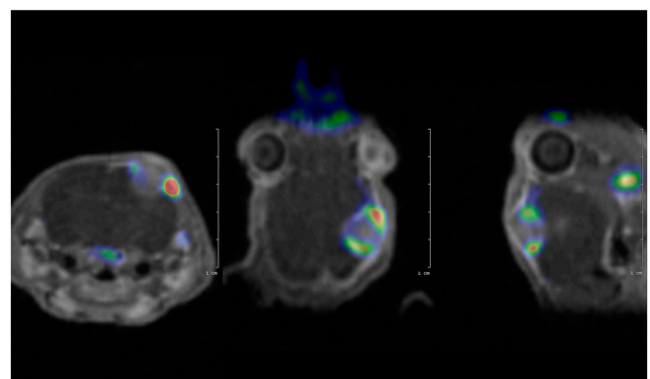
The clinical use of simultaneous SPECT/MRI to directly help assess (and thus predict) therapy monitoring will be most prominently present in the imaging and follow-up of local or systemic radionuclide therapy against post-surgical brain tumour remnants.^{74–76} Dosimetry and efficacy control will be possible with a SPECT/MRI system as opposed to PET/MRI, given that therapeutic nuclides are mostly SPECT emitters too. Improved dosimetry in the tumour is indispensable to optimize radionuclide therapeutic procedures for reaching the highest possible tumour dose. Improved regional dosimetry is necessary to identify dose-related organ impairment risks too.

There is further potential for future use of specific radionuclide-labelled peptides in targeted radionuclide therapy; provided that single photon emission is present in either the therapeutic radionuclide or an available analogue, then patient-specific dosimetry can be readily estimated. This would be an ideal use of the SPECT/MRI combination. In the future, one can anticipate availability of compounds that are labelled either with gamma emitters for diagnostic purposes or with therapeutic radionuclides; the ability to plan and monitor therapy with these paired compounds has potential. If used for therapy, the compound would be labelled with an alpha or beta emitter rather than a gamma emitter; the gamma version would be used to plan subsequent personalized therapy using the alpha or beta emitter. One case is with ¹³¹I-labelled compounds; ¹²³I labelling

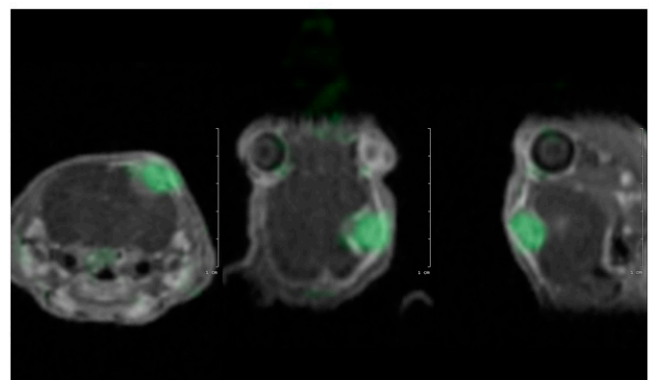
can be used instead for therapy planning. The alternative use of ¹²⁴I with PET is methodologically challenging and is limited by both general availability and dosimetric issues. One emerging example is targeted alpha therapy using ²¹²Pb, where ²⁰³Pb is proposed to be the surrogate dosimetry probe based on SPECT imaging.⁷⁷

Additional applications can be envisioned in research of the central nervous system. Functional MRI brain mapping studies combined with complementary, simultaneous SPECT readouts of neuroreceptor pathways using radio-labelled receptor ligands will be feasible with the system, although PET/MRI will probably remain the preferred modality for these studies. In treatment of diseases of the central nervous system (especially dementia), intensive development of new therapies is under way. SPECT/

Figure 10. (a) ^{99m}Tc-labelled pentavalent dimercaptosuccinic acid [^{99m}Tc-DMSA(V)] and gadolinium (Gd)-enhanced gradient-echo three-dimensional (3D) sequence MRI visualizes peripheral, more perfused regions of the tumour to express more transporter proteins of phosphate ions related to energy metabolism. Also, the superior nature of SPECT/MRI with very high resolution and high soft-tissue details/MRI-related functionality of the perfusion data readout is presented. (b) ¹²⁵I-deoxy-uridine and Gd-enhanced gradient-echo 3D sequence MRI visualizes central, less perfused regions of the tumour to express more DNA build-up (nucleoside incorporation). This image was taken synchronously with ^{99m}Tc-DMSA(V) images using an energy window centred at 28 keV.



(a)



(b)

MRI offers an outstanding opportunity for simultaneous blood perfusion imaging and determination of other disease indices such as dopamine transporter or neuroinflammation-associated parameters. Here, Go/No-Go decisions of large investments (in pharmaceutical discovery and development) are dependent on early disease detection and the evaluation of treatment effect. But, as suitable therapies are developed, the demand for cost-effective tools will increase; SPECT/MRI may be the system of choice for wider scale screening that may be indicated.

DISCUSSION

There are several potential advantages offered by simultaneous acquisition of MRI and SPECT images, rather than simply sequential acquisition *via* adjacent gantries (or totally independent acquisition). The reduction of the overall scan time and associated improvements in patient comfort and compliance are important. The availability of registered data sets to assist localization can be helpful, as it is not always possible with separately acquired modalities, especially with highly specific radiotracers where many structures may not be visualized. However, the potential to combine information from the two modalities so as to enhance diagnostic and prognostic information is particularly appealing. This can potentially extend beyond the improvement of SPECT quantification *via* motion or partial volume correction (PVC) to the development of joint models that might enhance both SPECT- and MRI-derived parameters. There is a strong case to evaluate the potential of this new multimodality option.

Both SPECT and MRI are lengthy procedures requiring patient cooperation, but restricting motion for lengthy periods can be a challenge, especially with certain brain conditions where movement control is affected. Motion effects can therefore be significant. Monitoring motion during SPECT acquisition is therefore very important and will allow correction of motion during reconstruction; this does imply that motion can be sufficiently well monitored during the complete SPECT acquisition,

which should be possible using techniques being developed for PET/MRI.^{78–80} For example, MRI navigator techniques can monitor and correct for motion for predefined regions such as the surface of the head, acquired in combination with most standard MRI techniques that may be selected for clinical studies (*e.g.* T_1 , T_2). There are, however, challenges in accurately determining the rigid motion based on six degrees of freedom and alternative methods of motion tracking may be more appropriate, provided these can be implemented in the practical setting, with minimal interference to the normal clinically indicated MRI acquisition.

Much of the work on PVC has been developed for PET. Traditionally, in the case of clinical systems, SPECT resolution is inferior to that of PET. PVC for SPECT is therefore more demanding but critical. Once again, the techniques that have been developed for PET/MRI are easily adapted for the SPECT/MRI application. The availability of simultaneous SPECT and MRI data will greatly facilitate correction using post-reconstruction methods,⁸¹ potentially reducing registration errors that affect PVC accuracy.

A distinct advantage of SPECT over PET is the potential for simultaneous acquisition of multiple radiotracers labelled with different radionuclides. Similar techniques in PET rely on sequential use of short half-life radionuclides and extrapolation of time–activity curves. The ability to combine multitracer studies with multiple MRI pulse sequences extends the potential to better characterize tissue and evaluate treatment. A preclinical example of combined multi-radionuclide imaging and MRI is illustrated in Figure 10. Dual radionuclide imaging does require corrections for downscatter, scattered photons from the higher energy emitter that are acquired in the energy window selected for the lower energy radionuclide. Correction is more complex in the case of CZT, where a tail in the energy spectrum due to incomplete charge collection must also be accounted for.^{82–84} A range of radiopharmaceuticals may be of interest for dual radionuclide imaging (Table 1).

Table 1. Possible measurements using SPECT/MRI including a range of MRI biomarkers along with ^{99m}Tc -labelled compounds and additional compounds with second radionuclide, which could be used interchangeably

MRI	Application	SPECT1	Application 1	SPECT2	Application 2
T_1 , gadolinium enhancement	Tumour site, blood–brain barrier integrity	^{99m}Tc -DMSA(V)	Phosphate transport	^{201}Tl -chloride	Perfusion/glia activity (prognosis)
T_2 + FLAIR	Invasiveness	^{99m}Tc -DTPA	Blood–brain barrier integrity	^{111}In -RGD peptide	Angiogenesis
MRI perfusion + T_2 FLAIR	Invasiveness, oedema	^{99m}Tc -Annexin-V	Apoptosis	^{123}I -CLINDE	Histologic classification
DWI + ADC additive: DTI	Intracellular/extracellular oedema, pseudoprogression	^{99m}Tc -HMPAO	Perfusion	^{111}In -Nimotuzumab	Planning for specific treatment
MR spectroscopy	Histologic classification	^{99m}Tc -HL91	Hypoxia	^{123}I -iodoUracyl	Proliferation post-therapy

ADC, apparent diffusion coefficient; DTI, diffusion tensor imaging; DWI, diffusion weighted imaging; FLAIR, fluid-attenuated inversion recovery; ^{123}I -CLINDE, ^{123}I -labelled 6-chloro-2-(4'-iodophenyl)-3-(*N,N*-diethyl)imidazo[1,2-*a*]pyridine-3-acetamide; ^{111}In -labelled arginyl-glycyl-aspartic acid (RGD) peptide; SPECT, single-photon emission computed tomography; ^{99m}Tc -DMSA(V), ^{99m}Tc -labelled pentavalent dimercaptosuccinic acid; ^{99m}Tc -DTPA, ^{99m}Tc -labelled diethylenetriaminepentaacetic acid; ^{99m}Tc -HL91, ^{99m}Tc -labelled 4,9-diaza-3,3,10,10-tetramethyldecane-2,11-dione dioxime; ^{99m}Tc -HMPAO, ^{99m}Tc -labelled hexamethylpropyleneamine oxime.

Potential diversity of simultaneous measurement in the context of tumour characterization is well illustrated.

There is still much to do to reach a stage of demonstrating robustness of SPECT/MRI and evaluating its clinical utility. Whether solid-state detectors or SiPM readout systems will become the design of choice remains to be seen. Extension of design ideas to permit whole-body acquisition may require a larger bore than typical of current MRI systems. Wide bore systems are clinically appealing to ease patient access and improve patient comfort; so, this MRI system development may be dictated by independent clinical demands. Early experience suggests that clinical performance similar to that available on conventional SPECT systems should be possible with relatively compact detector/collimator combinations, although further innovation may be needed to address sampling issues when the FOV is enlarged to accommodate the whole body.

CONCLUSION

The combination of SPECT and MRI is currently absent from the range of clinical multimodality systems, although work is in progress to produce the first prototype. As in the case of PET/

MRI, the combination of SPECT and MRI is attractive to patients who often have to undergo multiple lengthy imaging procedures. The dual radionuclide capability has particular appeal, although the clinical need for a simultaneous SPECT/MRI acquisition remains to be demonstrated. The development of appropriate technology remains challenging, but ultimately may lead to more general superior SPECT performance.

ACKNOWLEDGMENTS

This work was supported by a European Union Seventh Framework Program FP7/2007-2013 under project INSERT (HEALTH-F5-2012-305311). DM and NK also receive support from FP7/2007-2013 project INMiND (278850). DS is supported by the Portuguese national funding agency for science, research and technology (SFRH/BD/88093/2012). Researchers at the UCL Institute of Nuclear Medicine receive support from the National Institute of Health Research University College London Hospitals Biomedical Research Centre.

REFERENCES

- Patton JA, Townsend DW, Hutton BF. Hybrid imaging technology: from dreams and vision to clinical devices. *Semin Nucl Med* 2009; **39**: 247–63. doi: <https://doi.org/10.1053/j.semnuclmed.2009.03.005>
- Pichler BJ, Wehrl HF, Kolb A, Judenhofer MS. Positron emission tomography/magnetic resonance imaging: the next generation of multimodality imaging? *Semin Nucl Med* 2008; **38**: 199–208. doi: <https://doi.org/10.1053/j.semnuclmed.2008.02.001>
- Cherry SR, Louie AY, Jacobs RE. The integration of positron emission tomography with magnetic resonance imaging. *Proc IEEE* 2008; **96**: 416–38. doi: <https://doi.org/10.1109/jproc.2007.913502>
- Zaidi H, Del Guerra A. An outlook on future design of hybrid PET/MRI systems. *Med Phys* 2011; **38**: 5667–89. doi: <https://doi.org/10.1118/1.3633909>
- Pichler BJ, Judenhofer MS, Catana C, Walton JH, Kneilling M, Nutt RE, et al. Performance test of an LSO-APD detector in a 7-T MRI scanner for simultaneous PET/MRI. *J Nucl Med* 2006; **47**: 639–47.
- McElroy DP, Saveliev V, Reznik A, Rowlands JA. Evaluation of silicon photomultipliers: a promising new detector for MR compatible PET. *Nucl Instrum Methods Phys Res Sect A* 2007; **571**: 106–9. doi: <https://doi.org/10.1016/j.nima.2006.10.040>
- Meng LJ, Tan J-W, Fu G. Design study of an MRI compatible ultra-high resolution SPECT for *in vivo* mice brain imaging. Nuclear Science Symposium Conference Record. 2007 NSS '07 IEEE; 2007. 26 October 2007 to 3 November 2007.
- Hamamura MJ, Ha S, Roeck WW, Muftuler LT, Wagenaar DJ, Meier D, et al. Development of an MR-compatible SPECT system (MRSPECT) for simultaneous data acquisition. *Phys Med Biol* 2010; **55**: 1563–75. doi: <https://doi.org/10.1088/0031-9155/55/6/002>
- Cai L, Meng LJ. Hybrid pixel-waveform CdTe/CZT detector for use in an ultrahigh resolution MRI compatible SPECT system. *Nucl Instrum Methods Phys Res A* 2013; **702**: 101–103. doi: <https://doi.org/10.1016/j.nima.2012.08.069>
- Schlemmer HP, Pichler BJ, Schmand M, Burbar Z, Michel C, Ladebeck R, et al. Simultaneous MR/PET imaging of the human brain: feasibility study. *Radiology* 2008; **248**: 1028–35. doi: <https://doi.org/10.1148/radiol.2483071927>
- Delso G, Fürst S, Jakoby B, Ladebeck R, Ganter C, Nekolla SG, et al. Performance measurements of the Siemens mMR integrated whole-body PET/MR scanner. *J Nucl Med* 2011; **52**: 1914–22. doi: <https://doi.org/10.2967/jnumed.111.092726>
- Mackewn JE, Halsted P, Charles-Edwards G, Page R, Totman JJ, Sunassee K, et al. Performance evaluation of an MRI-compatible pre-clinical PET system using long optical fibers. *IEEE Trans Nucl Sci* 2010; **57**: 1052–62. doi: <https://doi.org/10.1109/tns.2010.2044891>
- Yamamoto S, Watabe H, Kanai Y, Watabe H, Hatazawa J. Development of an optical fiber-based MR compatible gamma camera for SPECT/MRI systems. *IEEE Trans Nucl Sci* 2015; **62**: 76–81. doi: <https://doi.org/10.1109/tns.2014.2387432>
- Wagenaar DJ, Kapusta M, Li J, Patt BE. Rationale for the combination of nuclear medicine with magnetic resonance for pre-clinical imaging. *Technol Cancer Res Treat* 2006; **5**: 343–50. doi: <https://doi.org/10.1177/153303460600500406>
- Hawkes R, Lucas A, Stevick J, Llosa G, Marcatili S, Piemonte C, et al. Silicon photomultiplier performance tests in magnetic resonance pulsed fields. Nuclear Science Symposium Conference Record. 2007 NSS '07 IEEE; 2007. 26 October 2007 to 3 November 2007.
- Nassalski A, Moszynski M, Syntfeld-Kazuch A, Szczesniak T, Swiderski L, Wolski D, et al. Silicon photomultiplier as an alternative for APD in PET/MRI applications. Nuclear Science Symposium Conference Record. 2008 NSS '08 IEEE; 2008. 19 October 2008 to 25 October 2008.
- Mendes PR, Cuervo R, Sarasola I, García de Acilu P, Navarrete J, Vela O, et al. A detector insert based on continuous scintillators for hybrid MR-PET imaging of the human brain. *Nucl Instrum Methods Phys Res Sect A* 2013; **702**: 80–2.
- Yamamoto S, Watabe H, Kanai Y, Watabe T, Kato K, Hatazawa J. Development of an ultrahigh resolution Si-PM based PET system for small animals. *Phys Med Biol* 2013; **58**: 7875–88. doi: <https://doi.org/10.1088/0031-9155/58/21/7875>
- David S, Georgiou M, Fysikopoulos E, Loudos G. Evaluation of a SiPM array coupled to a Gd₃Al₂Ga₃O₁₂:Ce (GAGG:Ce) discrete scintillator. *Phys Med* 2015; **31**: 763–6.

20. Schaart DR, Charbon E, Frach T, Schulz V. Advances in digital SiPMs and their application in biomedical imaging. *Nucl Instrum Methods Phys Res Sect A* 2016; **809**: 31–52. doi: <https://doi.org/10.1016/j.nima.2015.10.078>
21. Meier D, Mikkelsen S, Talebi J, Azman S, Maehlum G, Patt BE. An ASIC for SiPM/MPPC readout. IEEE Nuclear Science Symposium & Medical Imaging Conference; 2010. 30 October 2010 to 6 November 2010.
22. Cai L, Lai X, Shen Z, Chen CT, Meng LJ. MRC-SPECT: a sub-500 μm resolution MR-compatible SPECT system for simultaneous dual-modality study of small animals. *Nucl Instrum Methods Phys Res A* 2014; **734**: 147–51. doi: <https://doi.org/10.1016/j.nima.2013.08.080>
23. Erlandsson K, Kacperski K, van Gramberg D, Hutton BF. Performance evaluation of D-SPECT: a novel SPECT system for nuclear cardiology. *Phys Med Biol* 2009; **54**: 2635–49. doi: <https://doi.org/10.1088/0031-9155/54/9/003>
24. Bocher M, Blevins IM, Tsukerman L, Shrem Y, Kovalski G, Volokh L. A fast cardiac gamma camera with dynamic SPECT capabilities: design, system validation and future potential. *Eur J Nucl Med Mol Imaging* 2010; **37**: 1887–902. doi: <https://doi.org/10.1007/s00259-010-1488-z>
25. Hruska CB, Phillips SW, Whaley DH, Rhodes DJ, O'Connor MK. Molecular breast imaging: use of a dual-head dedicated gamma camera to detect small breast tumors. *AJR Am J Roentgenol* 2008; **191**: 1805–15. doi: <https://doi.org/10.2214/AJR.07.3693>
26. Keidar Z, Raysberg I, Lugassi R, Frenkel A, Israel O. Novel cadmium zinc telluride based detector general purpose gamma camera: initial evaluation and comparison with a standard camera. *J Nucl Med* 2016; **57**(Suppl. 2): 259.
27. Bisogni MG, Morrocchi M. Development of analog solid-state photo-detectors for Positron Emission Tomography. *Nucl Instrum Methods Phys Res Sect A* 2016; **809**: 140–48. doi: <https://doi.org/10.1016/j.nima.2015.09.114>
28. Roncali E, Cherry SR. Application of silicon photomultipliers to positron emission tomography. *Ann Biomed Eng* 2011; **39**: 1358–77. doi: <https://doi.org/10.1007/s10439-011-0266-9>
29. Quick HH. Integrated PET/MR. *J Magn Reson Imaging* 2014; **39**: 243–58. doi: <https://doi.org/10.1002/jmri.24523>
30. Delso G, Khalighi M, Hofbauer M, Porto M, Veit-Haibach P, von Schulthess G. Preliminary evaluation of image quality in a new clinical ToF-PET/MR scanner. *EJNMMI Phys* 2014; **1**(Suppl. 1): A41. doi: <https://doi.org/10.1186/2197-7364-1-S1-A41>
31. Yamamoto S, Watabe H, Kanai Y, Imaizumi M, Watabe T, Shimosegawa E, et al. Development of a high-resolution Si-PM-based gamma camera system. *Phys Med Biol* 2011; **56**: 7555–67. doi: <https://doi.org/10.1088/0031-9155/56/23/014>
32. Bouckaert C, Vandenberghe S, Van Holen R. Evaluation of a compact, high-resolution SPECT detector based on digital silicon photomultipliers. *Phys Med Biol* 2014; **59**: 7521–39. doi: <https://doi.org/10.1088/0031-9155/59/23/7521>
33. Dinu N, Imando TA, Nagai A, Pinot L, Puill V, Callier S, et al. SiPM arrays and miniaturized readout electronics for compact gamma camera. *Nucl Instrum Methods Phys Res Sect A* 2015; **787**: 367–72. doi: <https://doi.org/10.1016/j.nima.2015.01.083>
34. Philippov D, Ilyin A, Belyaev V, Popova E, Buzhan P, Stifutkin A. SiPM-MAROC gamma-camera prototype with monolithic NaI(Tl) scintillator. *EJNMMI Phys* 2015; **2**(Suppl. 1): A49. doi: <https://doi.org/10.1186/2197-7364-2-S1-A49>
35. Rogulski MM, Barber HB, Barrett HH, Shoemaker RL, Woolfenden JM. Ultra-high-resolution brain SPECT imaging: simulation results. *IEEE Trans Nucl Sci* 1993; **40**: 1123–29.
36. Goorden MC, Rentmeester MC, Beekman FJ. Theoretical analysis of full-ring multipinhole brain SPECT. *Phys Med Biol* 2009; **54**: 6593–610. doi: <https://doi.org/10.1088/0031-9155/54/21/010>
37. Salvado D, Erlandsson K, Bousse A, Occhipinti M, Busca P, Fiorini C, et al. Collimator design for a brain SPECT/MRI insert. *IEEE Trans Nucl Sci* 2015; **62**: 1716–24. doi: <https://doi.org/10.1109/tns.2015.2450017>
38. Busca P, Occhipinti M, Trigilio P, Cozzi G, Fiorini C, Piemonte C, et al. Experimental evaluation of a SiPM-based scintillation detector for MR-compatible SPECT systems. *IEEE Trans Nucl Sci* 2015; **62**: 2122–8. doi: <https://doi.org/10.1109/tns.2015.2481184>
39. Goetz C, Breton E, Choquet P, Israel-Jost V, Constantinesco A. SPECT low-field MRI system for small-animal imaging. *J Nucl Med* 2008; **49**: 88–93. doi: <https://doi.org/10.2967/jnumed.107.044313>
40. Tsui B, Xu J, Rittenbach A, El-Sharkawy AM, Edelstein W, Liu A, et al. The development of a high-resolution insert for simultaneous SPECT-MR imaging of small animals. *Soc Nucl Med Annu Meet Abstr* 2012; **53**(Suppl. 1): 2401.
41. Tsui B, Xu J, Rittenbach A, El-Sharkawy AM, Edelstein W, Parnham K, et al. A completed SPECT/MR insert for simultaneous SPECT/MR imaging of small animals. *Soc Nucl Med Annu Meet Abstr* 2013; **54**(Suppl. 2): 595.
42. Tsui BMW, Jingyan X, Rittenbach A, Si C, El-Sharkawy A, Edelstein WA, et al. High performance SPECT system for simultaneous SPECT-MR imaging of small animals. Nuclear science symposium and medical imaging conference (NSS/MIC). 2011 IEEE; 2011, 23 October 2011 to 29 October 2011.
43. Deprez K, Van Holen R, Vandenberghe S. A high resolution SPECT detector based on thin continuous LYSO. *Phys Med Biol* 2014; **59**: 153–71. doi: <https://doi.org/10.1088/0031-9155/59/1/153>
44. Occhipinti M, Busca P, Butt AD, Cozzi G, Fiorini C, Perali I, et al. A compact SiPM photodetector array for SPECT applications. 2014 IEEE nuclear science symposium and medical imaging conference (NSS/MIC); 2014. 8 November 2014 to 15 November 2014.
45. Van Audenhaege K, Vandenberghe S, Deprez K, Vandeghinste B, Van Holen R. Design and simulation of a full-ring multi-lofthole collimator for brain SPECT. *Phys Med Biol* 2013; **58**: 6317–36. doi: <https://doi.org/10.1088/0031-9155/58/18/6317>
46. Van Holen R, Vandenberghe S. Optimization of a stationary small animal SPECT system for simultaneous SPECT/MRI. Nuclear science symposium and medical imaging conference (NSS/MIC), 2013 IEEE; 2013. 27 October 2013 to 2 November 2013.
47. Van Audenhaege K, Van Holen R, Vandenberghe S, Vanhove C, Metzler SD, Moore SC. Review of SPECT collimator selection, optimization, and fabrication for clinical and preclinical imaging. *Med Phys* 2015; **42**: 4796–813. doi: <https://doi.org/10.1118/1.4927061>
48. Samoudi AM, Van Audenhaege K, Vermeeren G, Verhoyen G, Martens L, Van Holen R, et al. Simulated design strategies for SPECT collimators to reduce the eddy currents induced by MRI gradient fields. *IEEE Trans Nucl Sci* 2015; **62**: 2017–22. doi: <https://doi.org/10.1109/tns.2015.2476601>
49. Crozier S, Eccles CD, Beckey FA, Field J, Doddrell DM. Correction of eddy-current-induced B0 shifts by receiver reference-phase modulation. *J Magn Reson* 1992; **97**: 661–65. doi: [https://doi.org/10.1016/0022-2364\(92\)90049-d](https://doi.org/10.1016/0022-2364(92)90049-d)
50. Miller BW, Moore JW, Barrett HH, Frye T, Adler S, Sery J, et al. 3D printing in X-ray and gamma-ray imaging: a novel method for fabricating high-density imaging apertures. *Nucl Instrum Methods Phys Res A* 2011; **659**: 262–8. doi: <https://doi.org/10.1016/j.nima.2011.08.051>
51. Samoudi AM, Van Audenhaege K, Vermeeren G, Poole M, Tanghe E, Martens L, et al. Analysis of eddy currents induced by

- transverse and longitudinal gradient coils in different tungsten collimators geometries for SPECT/MRI integration. *Magn Reson Med* 2015; **74**: 1780–9. doi: <https://doi.org/10.1002/mrm.25534>
52. Deprez K, Vandenberghe S, Van Audenhaege K, Van Vaerenbergh J, Van Holen R. Rapid additive manufacturing of MR compatible multipinhole collimators with selective laser melting of tungsten powder. *Med Phys* 2013; **40**: 012501. doi: <https://doi.org/10.1118/1.4769122>
 53. Shellock FG. Metallic surgical instruments for interventional MRI procedures: evaluation of MR safety. *J Magn Reson Imaging* 2001; **13**: 152–7. doi: [https://doi.org/10.1002/1522-2586\(200101\)13:1<152::AID-JMRI1023>3.0.CO;2-C](https://doi.org/10.1002/1522-2586(200101)13:1<152::AID-JMRI1023>3.0.CO;2-C)
 54. Shellock FG. Compatibility of an endoscope designed for use in interventional MR imaging procedures. *AJR Am J Roentgenol* 1998; **171**: 1297–300. doi: <https://doi.org/10.2214/ajr.171.5.9798866>
 55. Shellock FG, Crues JV. High-field-strength MR imaging and metallic biomedical implants: an *ex vivo* evaluation of deflection forces. *AJR Am J Roentgenol* 1988; **151**: 389–92. doi: <https://doi.org/10.2214/ajr.151.2.389>
 56. Shellock FG, Shellock VJ. Ceramic surgical instruments: *ex vivo* evaluation of compatibility with MR imaging at 1.5 T. *J Magn Reson Imaging* 1996; **6**: 954–6. doi: <https://doi.org/10.1002/jmri.1880060620>
 57. ASTM International, West Conshohocken, PA, 2015, <https://doi.org/10.1520/F2052-15>
 58. ASTM International, West Conshohocken, PA, 2013, <https://doi.org/10.1520/F2119-07R13>
 59. ASTM International, West Conshohocken, PA, 2011, <https://doi.org/10.1520/F2182-11A>
 60. ASTM International, West Conshohocken, PA, 2011, <https://doi.org/10.1520/F2213-06R11>
 61. Medical Device Directive 93/42/EEC. 14 June 1993.
 62. IEC. 60601–1 medical electrical equipment-part 1: general requirements for basic safety and essential performance. edn 3.0 2005-12.
 63. IEC. 60601-2-33 Medical electrical equipment-part 2-33: particular requirements for the basic safety and essential performance of magnetic resonance equipment for medical diagnosis. edn 3.0 2010.
 64. Schenck JF. The role of magnetic susceptibility in magnetic resonance imaging: MRI magnetic compatibility of the first and second kinds. *Med Phys* 1996; **23**: 815–50. doi: <https://doi.org/10.1118/1.597854>
 65. Wendt O. Entwicklung einer spulenintegrierten und automatisch gesteuerten Biopsieeinrichtung zur histologischen Abklärung von Kleintumoren in der MR-Mammadiagnostik: Medizinische Fakultät—Universitätsklinikum Charité; 2004.
 66. Schaefer G. Testing MR safety and compatibility: an overview of the methods and current standards. *IEEE Eng Med Biol Mag* 2008; **27**: 23–7. doi: <https://doi.org/10.1109/EMB.2007.910267>
 67. Nyenhuis J, Kildishev AV, Bourland JD, Foster KS, Graber G, Athey TW. Heating near implanted medical devices by the MRI RF-magnetic field. *IEEE Trans Magn* 1999; **35**: 4133–35. doi: <https://doi.org/10.1109/20.800779>
 68. IEC. Medical electrical equipment. Part 2–33: particular requirements for the safety of magnetic resonance equipment for medical diagnosis; 2015. 60601-2-33 edn 3.2.
 69. Graessl A, Renz W, Hezel F, Dieringer MA, Winter L, Oezderm C, et al. Modular 32-channel transceiver coil array for cardiac MRI at 7.0T. *Magn Reson Med* 2014; **72**: 276–90. doi: <https://doi.org/10.1002/mrm.24903>
 70. Thalhammer C, Renz W, Winter L, Hezel F, Rieger J, Pfeiffer H, et al. Two-dimensional sixteen channel transmit/receive coil array for cardiac MRI at 7.0 T: design, evaluation, and application. *J Magn Reson Imaging* 2012; **36**: 847–57. doi: <https://doi.org/10.1002/jmri.23724>
 71. Pope WB, Sayre J, Perlina A, Villablanca JP, Mischel PS, Cloughesy TE. MR imaging correlates of survival in patients with high-grade gliomas. *AJNR Am J Neuroradiol* 2005; **26**: 2466–74.
 72. Grosu AL, Astner ST, Riedel E, Nieder C, Wiedenmann N, Heinemann F, et al. An interindividual comparison of O-(2-[18F]fluoroethyl)-L-tyrosine (FET)- and L-[methyl-11C]methionine (MET)-PET in patients with brain gliomas and metastases. *Int J Radiat Oncol Biol Phys* 2011; **81**: 1049–58. doi: <https://doi.org/10.1016/j.ijrobp.2010.07.002>
 73. Galldiks N, Dunkl V, Stoffels G, Hutterer M, Rapp M, Sabel M, et al. Diagnosis of pseudoprogression in patients with glioblastoma using O-(2-[18F]fluoroethyl)-L-tyrosine PET. *Eur J Nucl Med Mol Imaging* 2015; **42**: 685–95. doi: <https://doi.org/10.1007/s00259-014-2959-4>
 74. Carollo A, Papi S, Chinol M. Lutetium-177 labeled peptides: the European Institute of Oncology Experience. *Curr Radiopharm* 2016; **9**: 19–32. doi: <https://doi.org/10.2174/1874471008666150313111633>
 75. Cordier D, Forrer F, Kneifel S, Sailer M, Mariani L, Macke H, et al. Neoadjuvant targeting of glioblastoma multiforme with radiolabeled DOTAGA-substance P—results from a phase I study. *J Neurooncol* 2010; **100**: 129–36. doi: <https://doi.org/10.1007/s11060-010-0153-5>
 76. Reardon DA, Zalutsky MR, Akabani G, Coleman RE, Friedman AH, Herndon JE 2nd, et al. A pilot study: 131I-antitnascin monoclonal antibody 81c6 to deliver a 44-Gy resection cavity boost. *Neuro Oncol* 2008; **10**: 182–9. doi: <https://doi.org/10.1215/15228517-2007-053>
 77. Máthé D, Szigeti K, Hegedűs N, Horváth I, Veres DS, Kovács B, et al. Production and *in vivo* imaging of (203)Pb as a surrogate isotope for *in vivo* (212)Pb internal absorbed dose studies. *Appl Radiat Isot* 2016; **114**: 1–6. doi: <https://doi.org/10.1016/j.apradiso.2016.04.015>
 78. Catana C, Drzezga A, Heiss WD, Rosen BR. PET/MRI for neurologic applications. *J Nucl Med*. 2012; **53**: 1916–25. doi: <https://doi.org/10.2967/jnumed.112.105346>
 79. Ullisch MG, Scheins JJ, Weirich C, Rota Kops E, Celik A, Tellmann L, et al. MR-based PET motion correction procedure for simultaneous MR-PET neuroimaging of human brain. *PLoS One* 2012; **7**: e48149. doi: <https://doi.org/10.1371/journal.pone.0048149>
 80. Keller SH, Hansen C, Hansen C, Andersen FL, Ladefoged C, Svarer C, et al. Motion correction in simultaneous PET/MR brain imaging using sparsely sampled MR navigators: a clinically feasible tool. *EJNMMI Phys* 2015; **2**: 14. doi: <https://doi.org/10.1186/s40658-015-0118-z>
 81. Erlandsson K, Buvat I, Pretorius PH, Thomas BA, Hutton BF. A review of partial volume correction techniques for emission tomography and their applications in neurology, cardiology and oncology. *Phys Med Biol* 2012; **57**: R119–59. doi: <https://doi.org/10.1088/0031-9155/57/21/r119>
 82. Kacperski K, Erlandsson K, Ben-Haim S, Hutton BF. Iterative deconvolution of simultaneous 99mTc and 201Tl projection data measured on a CdZnTe-based cardiac SPECT scanner. *Phys Med Biol* 2011; **56**: 1397–414. doi: <https://doi.org/10.1088/0031-9155/56/5/012>
 83. Fan P, Hutton BF, Holstenson M, Ljungberg M, Pretorius PH, Prasad R, et al. Scatter and crosstalk corrections for 99mTc/123I dual-radionuclide imaging using a CZT SPECT system with pinhole collimators. *Med Phys* 2015; **42**: 6895–911. doi: <https://doi.org/10.1118/1.4934830>
 84. Holstenson M, Erlandsson K, Poludniowski G, Ben-Haim S, Hutton BF. Model-based correction for scatter and tailing effects in simultaneous 99mTc and 123I imaging for a CdZnTe cardiac SPECT camera. *Phys Med Biol* 2015; **60**: 3045–63. doi: <https://doi.org/10.1088/0031-9155/60/8/3045>